The Cryosphere Discuss., 8, 6007–6032, 2014
www.the-cryosphere-discuss.net/8/6007/2014/
doi:10.5194/tcd-8-6007-2014

The Cryosphere Discussions
Open Access

Comparison of aeolian snow transport events and snow mass fluxes between observations and simulations made by the regional climate model MAR in Adélie Land, East Antarctica

A. Trouvilliez[1,2,3,4], H. Gallée[1], F. Naaim-Bouvet[2,4], C. Genthon[1], C. Amory[1,2,4], V. Favier[1], C. Agosta[5], L. Piard[1], and H. Bellot[2,4]

[1]CNRS, LGGE, UMR5183, 38401 Grenoble, France
[2]Irstea, UR ETNA, 38402 Saint-Martin d'Hères, France
[3]Cerema-DTecEMF, LGCE, 29280 Plouzané, France
[4]Univ. Grenoble Alpes, 38041 Grenoble, France
[5]University of Liège, Department of Geography, 4020 Liège, Belgium

Received: 29 September 2014 – Accepted: 5 November 2014 – Published: 5 December 2014

Correspondence to: A. Trouvilliez (alexandre.trouvilliez@gmail.com)

Published by Copernicus Publications on behalf of the European Geosciences Union.

Abstract

The regional climate model MAR including a coupled snow pack/aeolian snow transport parameterisation is compared with aeolian snow mass fluxes at a fine spatial resolution (5 km horizontally and 2 m vertically) and at a fine temporal resolution (30 min) over 1 month in Antarctica. Numerous feedbacks are taken into account in the MAR including the drag partitioning caused by the roughness elements. Wind speed is correctly simulated with a positive value of the Nash test (0.60 and 0.37) but the wind speeds above 10 m s^{-1} are underestimated. The aeolian snow transport events are correctly reproduced with a good temporal resolution except for the aeolian snow transport events with a particles' maximum height below 1 m. The simulated threshold friction velocity, calculated without snowfall, is overestimated. The simulated aeolian snow mass fluxes between 0 to 2 m have the same variations but are underestimated compared to the second-generation FlowCapt values and so is the simulated relative humidity at 2 m. This underestimation is not entirely due to the underestimation of the simulated wind speed. The MAR underestimates the aeolian snow quantity that pass through the first two meters by a factor ten compared to the second-generation FlowCapt value (13 990 kg m^{-1} and 151 509 kg m^{-1} respectively). It will conduct the MAR, with this parametrisation, to underestimate the effect of the aeolian snow transport on the Antarctic surface mass balance.

1 Introduction

Aeolian snow mass flux measurements in Antarctica reveal that a large amount of snow is transported by the wind (Budd, 1966; Mann et al., 2000; Trouvilliez et al., 2014; Wendler, 1989). The aeolian snow transport and its subsequent sublimation is probably a significant component of the surface mass balance of the Antarctic ice sheet (ASMB). Previous estimations of the contribution of aeolian snow transport to the ASMB using numerical models were reported to be around 10 % (Déry and Yau, 2002; Lenaerts et al., 2012a). Estimations can be modelled without any feedback of the transport or with an aeolian snow transport model coupled to a regional climate model. In the latter case, in addition to atmospheric conditions, snow properties influence the aeolian snow mass fluxes and several physical feedbacks of the aeolian transport of snow influence the atmospheric conditions as previously highlighted by Gallée et al. (2013). Indeed, aeolian structures such as sastrugi and dunes may appear and they in turn influence the atmospheric dynamics. The transport also increases the air density by the presence of airborne snow particles and also by cooling due to the sublimation of these airborne snow particles. Thus, this may reduce the turbulence in the surface boundary layer and contribute negatively to the snow erosion (Bintanja, 2000; Wamser and Lykossov, 1995).

As previously highlighted (Gallée et al., 2001; Lenaerts et al., 2012b), there are few reliable data on aeolian snow transport covering a long period with an hourly temporal resolution, making model evaluation in Antarctica difficult. One-dimensional (1-D) numerical models have been compared with aeolian snow transport events and transport rates in ideal cases (Xiao et al., 2000) or with observations (Lenaerts et al., 2010). The regional climate models are evaluated on the surface mass balance obtained with stake lines (Gallée et al., 2005; Lenaerts et al., 2012c). This is an integrative method, which comprises the integration of precipitation, run-off, sublimation, erosion/deposition and transport. Aeolian snow transport events simulated by regional climate models have been compared with remote sensing techniques as described in Palm et al. (2011) and with visual observations obtained in different polar stations (Lenaerts et al., 2012b) or with particle impact sensors (Lenaerts et al., 2012c). Aeolian snow mass flux measurements are even rarer and (Lenaerts et al., 2012b) could evaluate simulations only with annual transport rate values obtained from FlowCapt™ (Scarchilli et al., 2010), which overestimate the aeolian snow mass flux in its first version (Trouvilliez et al., 2014), and from an extrapolation of optical particle counter sensor measurements (Mann et al., 2000). Thus, model evaluations call for more detailed and reliable aeolian snow transport measurements in Antarctica to improve analyses.

TCD
8, 6007–6032, 2014

Here, we present a detailed comparison between simulation of the regional climate model MAR and data from a long aeolian snow transport observation campaign in Adélie Land, Antarctica (Trouvilliez et al., 2014). We focus on a 1 month period, January 2011, and a small domain. A similar study has already been conducted for the January 2010 period with the same regional climate model (Gallée et al., 2013). However, in the latter work, model outputs were compared with a single point of aeolian snow transport measurements using the first-generation FlowCapt^{TM}. These sensors detect the aeolian snow transport events well but fail to estimate the aeolian snow mass fluxes (Cierco et al., 2007; Naaim-Bouvet et al., 2010; Trouvilliez et al., 2014). Second-generation FlowCapt^{TM} have been installed since February 2010 at two new automatic weather and snow stations. Unlike its first-generation counterpart, the second-generation sensor is able to give a lower bound estimate of the aeolian snow mass fluxes (Trouvilliez et al., 2014). It allows a comparison to be made not only between the simulated and observed timing of the aeolian snow transport events but also between the simulated and observed aeolian snow mass fluxes, which was not the case previously.

In the next two sections (Sects. 2 and 3), we present the field data and the model used. Comparisons between measurements and modelling results are shown in Sect. 4. Finally, the results are discussed in the last section.

2 Field data

Observations were made in Adélie Land, East Antarctica (Fig. 1), where surface atmospheric conditions are well described at the French permanent station Dumont D'Urville (Favier et al., 2011). The coastal region is characterized by frequent and strong katabatic winds with a maximum wind speed of around 100 km inland (Parish and Wendler, 1991; Wendler et al., 1997). The wind is frequently associated with aeolian snow transport events (Prud'homme and Valtat, 1957; Trouvilliez et al., 2014) making Adélie Land an excellent place for aeolian snow transport observations. Furthermore, a 40 year accumulation dataset is available in Adélie Land and long-term stake measurements are still performed along a 150 km stake line (Agosta et al., 2012) and in erosion areas (Favier et al., 2011; Genthon et al., 2007). These data give access to the annual SMB in the area.

Several meteorological campaigns including aeolian snow transport measurements have already been performed in Adélie Land with mechanical traps (Garcia, 1960; Lorius, 1962; Madigan, 1929) or optical particle counter sensors (Wendler, 1989). However, none of the measurements in Adélie Land or elsewhere in Antarctica fulfils all the requirements for an in-depth evaluation of regional climate models. A new aeolian snow transport observation campaign, started in 2009, was designed to optimally evaluate models to the extent possible considering logistical difficulties and limitations (Trouvilliez et al., 2014).

Automatic weather and snow stations are installed that continuously measure wind speed and relative humidity at a 2 m height every 10 s. Half-hourly mean values are stored at each station. The stations are equipped with FlowCapt™, acoustic sensors designed to quantify the aeolian snow mass fluxes and to withstand the harsh polar environment. Two generations of FlowCapt™ exist and have been evaluated in the French Alps and in Antarctica (Trouvilliez et al., 2014). Both generations seem to be good detectors for the aeolian snow transport events. The first-generation fails to correctly estimate the snow mass flux with the constructor calibration or with a new calibration, whereas the second-generation sensor can give a lower bound estimate of the snow mass flux and a consistent relationship of the flux vs. the wind speed.

FlowCapt™ sensors are very robust and designed to be set up vertically. When the low end of the sensor lies close to the ground or when it is partially buried, the FlowCapt™ is able to detect the onset of the transport (saltation of the transport). Because the snowpack level changes during the year (Favier et al., 2011; Genthon et al., 2007), this sensor offers continuous observation, which is an advantage over single point measurement sensors. FlowCapt™ has a better temporal resolution than visual observations usually made every 6 h. Moreover, the ability of these sensors to detect events of small magnitude is particularly interesting, as satellite measurements can only detect blowing snow events whose snow particles lifted from the surface reach 20 m or more in the absence of clouds (Palm et al., 2011). In Adélie Land, aeolian snow transport events with a maximum particles' height below 4.5 m represent 17 % of the aeolian snow transport events (Trouvilliez et al., 2014). The ground and satellite observations are thus complementary.

For the period 2010–2013, three automatic weather and snow stations were set up along the logistic traverse to Dome C, at location points D3, D17 and D47. These stations allow for the documentation of distinct climatic conditions (Fig. 1). Three first-generation FlowCapt™ sensors were set up from 0 to 1, 1 to 2, and 2 to 3 m at D3 close to a classic automatic weather station. One second-generation FlowCapt™ is installed at D17 from 0 to 1 m on a 7 m mast with six levels of cup anemometers and thermo hygrometers (Fig. 2). Two second-generation sensors are located at D47 from 0 to 1 and 1 to 2 m coupled to a classic automatic weather station. The half-hourly mean aeolian snow mass flux is recorded for each FlowCapt™ and stored in the datalogger. Since we focus on the simulated and observed snow mass fluxes, the evaluation will be limited to the two stations equipped with a second-generation FlowCapt™, i.e. D17 and D47 (Table 1).

3 Model

The MAR is a coupled atmosphere/snowpack/aeolian snow transport regional climate model. The atmospheric dynamics are detailed in Gallée and Schayes (1994). They are based on the hydrostatic approximation of the primitive equations with the normalized pressure as vertical coordinate. The integration of the snowpack and aeolian snow transport sub-models has been described in Gallée et al. (2001) and an improved version, used here, is detailed in Gallée et al. (2013).

Numerous feedbacks are parameterized in the MAR, described in Gallée et al. (2013), such as the particle stabilization of the surface boundary layer as defined

Discussion Paper | Discussion Paper | Discussion Paper | Discussion Paper |

TCD

8, 6007–6032, 2014

Comparison of aeolian snow transport events and snow mass fluxes

A. Trouvilliez et al.

by Bintanja (2000). The sublimation of the blown particle is computed by the microphysical scheme and has an effect on the heat and moisture budgets in the layer where the sublimation occurs. Aeolian snow transport also has an effect on the radiative transfer through the atmosphere as it can change the atmospheric optical depth (Gallée and Gorodetskaya, 2010). Densification of the snowpack by the wind is included from the work of Kotlyakov (1961), i.e. the snow density increases with an increase in the wind speed and thus the threshold friction velocity will be higher.

The threshold friction velocity for a smooth surface depends on the snowpack characteristics: the dendricity, the sphericity and the grain size for density below 330 $\mathrm{kg\,m^{-3}}$ as in Guyomarc'h and Mérindol (1998), and the snow density above 330 $\mathrm{kg\,m^{-3}}$. To account for the drag partition caused by the roughness elements, the threshold friction velocity for a rough surface is calculated as in Marticorena and Bergametti (1995):

$$u_{*\mathrm{tR}} = \frac{u_{*\mathrm{tS}}}{R_\mathrm{f}} \tag{1}$$

Where $u_{*\mathrm{tR}}$ is the threshold friction velocity for a rough surface, $u_{*\mathrm{tS}}$ is the threshold friction velocity for a smooth surface and R_f is a ratio factor defined as:

$$R_\mathrm{f} = 1 - \left[\frac{\ln\left(\frac{z_{0\mathrm{R}}}{z_{0\mathrm{S}}}\right)}{\ln\left(0.35\left(\frac{10}{z_{0\mathrm{S}}}\right)^{0.8}\right)} \right] \tag{2}$$

where $z_{0\mathrm{R}}$ and $z_{0\mathrm{S}}$ are the surface roughness lengths for rough and smooth surfaces, respectively, in meters. The sensitivity of R_f to $z_{0\mathrm{S}}$ is small for a value of $z_{0\mathrm{S}}$ above 5×10^{-5} m (Marticorena and Bergametti, 1995). The general value of the roughness height of smooth snow cover is around 10^{-5}–10^{-4} m (Leonard et al., 2011). In additional to the drag partition, moving particles in the saltation layer transfer momentum from the airflow to the surface. Above the saltation layer, the net effect is similar to

TCD
8, 6007–6032, 2014

that of a stationary roughness element (Owen, 1964). Thus, saltation leads to an increase of the roughness length compared with the roughness length without transport even for a smooth surface. The z_{0S} is determined by a calibration with Byrd project measurements (Budd et al., 1966; Gallée et al., 2001):

$$z_{0S} = 5 \cdot 10^{-5} + \max\left(0.5 \cdot 10^{-6}, 0.536 \cdot 10^{-3} \cdot u_*^2 - 61.8 \cdot 10^{-6}\right) \tag{3}$$

One of the main roughness elements in the Antarctica snowpack is the sastrugi. They are profiled with the main wind direction, and a variation in the wind direction results in a change of the sastrugi drag coefficient and leads to an increase of the roughness height z_{0R} (Jackson and Carroll, 1978). Furthermore, the sastrugi adapt their profile to the new mean direction with a decrease of the coefficient drag to a limit value. Andreas (1995) estimates this time-response to be around half a day. Sastrugi can be buried if precipitation occurs. All these effects are taken into account in the improved version of the snowpack sub-model with the parameterization of the z_{0R} (Gallée et al., 2013), which is a negative feedback on the transport.

Once aeolian transport is initiated, the snow particles' concentration in the saltation layer, in kilograms of particle per kilograms of air, η_S , is parameterized from (Pomeroy, 1989):

$$\eta_S = \begin{cases} 0 & \text{if } u_{*R} < u_{*tR} \\ e_{\text{salt}}\left(\frac{u_{*R}^2 - u_{*tR}^2}{g \cdot h_{\text{salt}}}\right) & \text{if } u_{*R} \geq u_{*tR} \end{cases} \tag{4}$$

where u_{*R} is the friction velocity for a rough surface in $\mathrm{m\,s^{-1}}$, e_{salt} is the saltation efficiency equal to 3.25, g is the gravitational acceleration in $\mathrm{m\,s^{-2}}$ and h_{salt} is the saltation height in m, a function of u_{*R} (Pomeroy and Male, 1992).

TCD
8, 6007–6032, 2014

4 Comparison of field data and model

The aim of this section is to provide a detailed comparison between the observed and the modelled meteorological variables including relative humidity and aeolian snow mass fluxes. Modelling results are from a MAR simulation in Adélie Land during January 2011. A spin-up step, as described in Gallée et al. (2013), was applied for current modelling. The modelling grid and set-up are the same as those of Gallée et al. (2013): the integrative domain is a 450 km × 450 km square with a 5 km horizontal resolution (Fig. 1). Lateral forcing and sea-surface conditions are taken from ERA-Interim. There are 60 vertical levels with a first level at 2 m height and a vertical resolution of 2 m in the lowest 12 levels. The simulation started 1 month before the period of interest, i.e. 1 December 2010, in order to get a relative equilibrium of the snow pack with the atmospheric conditions. The model performances are assessed by the statistical test proposed by Nash and Sutcliffe (1970). An efficiency of 1 means a perfect simulation (RMSE = 0) and a value of 0 or less means that the model is not better than a minimalist model whose output constantly equals the mean value of the modelled variable over the studied time period.

The comparison focuses on the wind speed, as it is the driving force of aeolian transport. The timing of the aeolian snow transport events is then studied with an evaluation of the threshold friction velocity, and finally the aeolian snow mass fluxes are analysed. The relative humidity is also analysed to evaluate the aeolian snow transport sublimation. Indeed, it plays an important role in the ASMB (Lenaerts et al., 2012a) and it is crucial to evaluate numerical models at this point.

Wind speed and relative humidity are compared at a height of 2 m above the surface. Relative humidity with respect to the solid state is calculated from the expression of Goff and Gratch (1946). The observed values of aeolian snow mass fluxes from the FlowCapt$^{\text{TM}}$ in contact with the ground are compared with the values of simulated snow mass fluxes in the first layer (0–2 m) to assess the detection of aeolian snow transport events. The mean observed snow mass fluxes from 0 to 2 m are compared with the

TCD
8, 6007–6032, 2014

mean simulated snow mass flux from 0 to 2 m. As the lowest layer extends up to 2 m above the surface, the coarse resolution of the model does not allow simulations of the strong decrease of aeolian snow mass fluxes in the first meter, whereas 1-D simulation may do so with an affordable numerical time cost (Xiao et al., 2000). In order to correctly estimate the flux with the first level at 2 m, simulations from a 1-D model, with the same transport parameterization used in the 3-D MAR, were performed with different vertical resolutions. A dimensionless correction factor (A) is determined from these simulations:

$$\mu_{\mathrm{IC}} = \mu_{\mathrm{IR}} \cdot A = \mu_{\mathrm{IR}} \cdot \left[2 + 6 \cdot e^{(1.5 \cdot (2-0.4))}\right] \tag{5}$$

where μ_{IC} is the corrected flux for the lowest layer (0–2 m) and μ_{IR} the raw flux from the MAR for the lowest layer, both in $\mathrm{g\,m^{-2}\,s^{-1}}$. This correction is effective only if the MAR simulates aeolian snow transport event.

4.1 Wind speed

Wind speed is correctly simulated (Fig. 3), especially at D17, with an efficiency of 0.60 and 0.37, respectively, for D17 and D47. As already noted by Gallée et al. (2013), variations are correctly represented but wind speeds above $10\,\mathrm{m\,s^{-1}}$ are underestimated. This leads to a constant wind speed underestimation of $2\,\mathrm{m\,s^{-1}}$ at D47. This underestimation may be due to the E-ε turbulent scheme used in MAR. It is based on the small eddies concept and it cannot reproduce the large eddies responsible for the deflection of air parcels flowing higher in the boundary layer. The diagnostic wind gust model of Brasseur and Gallée (2002) is an adequate tool for representing the large eddies associated with high wind speeds and can be associated with the MAR outputs. Although the method simulates the wind gusts, it may be used as a tool with which to evaluate the mechanisms involved in the strong wind speed events. The wind gust amplitude simulated by this method corresponds to the maximum mean wind speed observed during strong wind speed events, which corroborates the hypothesis that the underestimation may come from the turbulent scheme.

TCD
8, 6007–6032, 2014

4.2 Aeolian snow transport events

We first compare the observed and simulated aeolian snow transport events. At D17 and D47 the observed snow mass fluxes from a FlowCapt^{TM} measuring snow particle impacts within a 0–1 m range above the surface are correctly simulated by the model except for the ones around 15 January at D17 (Fig. 3). During this event, the field reports mentioned that a strong snow transport event was observed, but was limited to the vicinity of the ground, i.e. below 1 m above the surface. This behaviour is confirmed by D47 data where a FlowCapt^{TM} is installed from 1 to 2 m. Indeed, the aeolian snow transport events with a maximum particles' height below 1 m above the surface are the only ones that the model is not able to correctly reproduce with a good temporal resolution (Fig. 3), probably because the lowest level of the model is situated 2 m above the surface.

The threshold friction velocities are evaluated at the D17 site as the friction velocity can be determined by the profile method (Garratt, 1992), which assumes a logarithmic profile of the wind speed. The friction velocities during January are calculated with the four upper cup anemometers with half-hourly wind speed (the two lowest cup anemometers were malfunctioning), as in Trouvilliez et al. (2014). Only regressions with a coefficient of determination above 0.98 are kept to ensure wind speed close to the logarithmic profile. During January 2011, the stratification of the atmosphere is for the most part near-neutral. The 95 % confidence limit of each friction velocity is determined for the statistical errors associated with the logarithmic profile (Wilkinson, 1984). The FlowCapt^{TM} in contact with the ground detects aeolian snow transport event: as soon as the flux value is above 0.001 $g\,m^{-2}\,s^{-1}$, the threshold friction velocity is calculated.

Threshold friction velocities cannot be determined experimentally when there is snowfall: the periods with snowfall have to be removed from the data for the threshold friction velocity evaluation. Thus, the ERA-interim data of the ECMWF are used, which seem to be the most reliable over the area (Palerme et al., 2014). The longest period without precipitation is between 13 and 19 January and will be used here (Fig. 4). During this period, six observed transport periods are identified and six observed threshold friction velocities are calculated (Fig. 4). However, during this period, MAR does not simulate any aeolian snow transport event. Generally, the simulated friction velocity is lower that the observed one. However, for three observed aeolian snow transport events (2, 3 and 5), the simulated friction velocity is higher than the upper 95 % confidence limit of the observed threshold friction velocity (considering a constant threshold friction velocity for each episode). The simulated threshold friction velocity is thus overestimated during this period.

4.3 Aeolian snow mass fluxes and relative humidity

The measured aeolian snow mass fluxes and relative humidity are now compared with the modelled ones (Fig. 5). The comparison is based only on the D47 Automatic Weather and Snow Station (AWSS), as this station gives information on the snow mass fluxes from 0 to 2 m above the surface, allowing a comparison to be made with the MAR model simulation. As previously observed, the MAR simulates aeolian snow transport events only when the particles' maximum height is above 1 m, and when it occurs, the MAR constantly underestimates the aeolian snow mass fluxes measured by the second-generation FlowCapt™, which already underestimates the snow mass flux (Trouvilliez et al., 2014). MAR also underestimates the relative humidity when observed aeolian snow transport events occur even in the first meter (Fig. 5). This underestimation may come from an underestimation of the blown snow particles' sublimation amount, related to the underestimation of the concentration of blown particles in the lower layer of the model.

The influence of the simulated wind speed underestimation on the simulated aeolian snow mass fluxes is assessed by comparing snow mass flux vs. wind speed for the four strong events that occurred during the month of study (Fig. 6). It is known that at a given height, for a given set of snow particles (i.e. the threshold friction velocity is constant during the episode), the aeolian transport of snow can be approximated by a power law of the wind speed (Mann et al., 2000; Radok, 1977). Such behaviour can clearly be identified for the observed snow mass flux during events 2, 3 and 4 (Fig. 6). For the first event, a hysteresis in the observed snow mass fluxes with the observed wind speed is recorded. Such a hysteresis effect has already been observed (Gordon et al., 2010). This observed variation may be due to a change in the erodible layers. Indeed, the snow mass flux–wind speed relationship presents three main behaviours through time (Fig. 4, upper left): the first one is characterised by a snow mass flux increase as the wind speed increases, the second one by a strong flux decrease at a nearly constant wind speed, and the third one by a flux decrease as the wind speed decreases but leading the same wind speed to be associated with higher aeolian snow mass flux than during the beginning of the event. It can be explained by the composition of the snowpack with an erodible surface layer, a harder intermediate layer below it with a higher threshold friction velocity, and a third layer, smoother than those above and thus easily erodible. The field reports do not offer additional information to verify this hypothesis and the MAR did not simulate it.

For the simulated snow mass fluxes, the largest occurred for a wind speed around $13\,\mathrm{m\,s^{-1}}$, clearly visible in the second and fourth events. Modelled fluxes first increase as modelled wind speed increases before the wind speed reaches a stable value, whereas the modelled fluxes continue to increase. This increase is due to the presence of strong simulated precipitations at that time. Thus, the precipitating particles are added to the previous blown snow particles from the surface and increase the aeolian snow mass flux, whereas the wind speed does not change. When the modelled wind speed decrease, so do the modelled fluxes.

Finally, MAR aeolian snow mass fluxes are twice lower than those provided by the second-generation FlowCapt$^{\mathrm{TM}}$ with the same wind speed values except when snowfall occurs. Thus, the underestimation of the simulated aeolian snow mass fluxes is not entirely due to the underestimation of the simulated wind speed. Furthermore, MAR is unable to reproduce the strong aeolian snow transport events with observed snow mass fluxes above $100\,\mathrm{g\,m^{-2}\,s^{-1}}$.

TCD
8, 6007–6032, 2014

Comparison of aeolian snow transport events and snow mass fluxes

A. Trouvilliez et al.

5 Discussion and conclusion

A regional climate model including a coupled snow pack/aeolian snow transport parameterisation is compared with aeolian snow mass fluxes at a fine spatial resolution (5 km horizontally and 2 m vertically) and at a fine temporal resolution (30 min) over 1 month in Antarctica. Several points of interest arose from this comparison. Firstly, the MAR reproduces the wind speed variations well but it underestimates the high wind speeds. This underestimation may be due to the turbulent scheme used based on the small eddies concept. Secondly, the occurrence of the aeolian snow transport events is well estimated except for those with a maximum particles' height below 1 m. This is probably due to the too-coarse vertical resolution of MAR near the surface. Indeed the first MAR level height is 2 m above the surface. This may also be linked to an overestimation of the threshold friction velocity by MAR. Thirdly, for the same wind speed, modelled snow mass fluxes are twice lower than the ones observed with the second-generation FlowCapt^{TM}. And it is known that the second-generation FlowCapt^{TM} already underestimates the snow mass fluxes of aeolian snow transport. Finally, the strong snow mass fluxes are not simulated. All these elements play a role and we found that the MAR-simulated snow quantity over the first 2 m at D47 over January is ten times lower than the one measured with the second-generation FlowCapt^{TM}: the MAR simulated 13 990 kg m^{-1} while the second-generation FlowCapt^{TM} recorded 151 509 kg m^{-1}. It will conduct the MAR to underestimate the aeolian snow transport effect on the Antarctic surface mass balance.

These differences in the amount of snow quantity between the FlowCapt^{TM} and the simulation may be justified by three different causes besides the underestimation of the wind speed above 10 m s^{-1} and the underestimation of the aeolian snow transport events. First, the saltation fluxes are based on the Pomeroy (Pomeroy, 1989) equation, which was observed to systematically underestimate accurate measurements of saltation snow mass fluxes (Doorschot and Lehning, 2002). This is not the case of the (Sørensen, 1991) formulation. The parameterization of the saltation transport rate with

TCD
8, 6007–6032, 2014

the (Sørensen, 1991) formulation may limit the underestimation in the simulation. Next, the drag partition is parameterized with a qualitative formulation (Gallée et al., 2013) based on the work of Jackson and Carroll (1978). In the case of an overestimation of the roughness height, it will lead to a deficit of shear stress available for snow erosion in the simulation and an overestimation of the threshold friction velocity. Considering Eq. (4), it leads also to an underestimation of the simulated snow mass fluxes. As the form drag is the main contributor to roughness height, a further calibration of the roughness height in the MAR is needed. Finally the densification process in the snowpack is based on the (Kotlyakov, 1961) formulation. An overestimation of the snow density will lead to an underestimation of the aeolian snow mass fluxes. Current observations cannot evaluate the simulated roughness height and snow density in the period of interest.

The comparison presented here is a step forward in the evaluation of the aeolian transport of snow by regional climate models. However, there are still processes to be evaluated and calibrated in the models that may be done with observations in simple atmospheric conditions such as in Antarctica compared with mountainous regions. Therefore, new observations are under way with roughness height and snow surface density measurements in Adélie Land. Furthermore, a comparison using remote sensing techniques, which give information on a large scale, and automatic weather and snow stations, which detect sensible small-magnitude events, will be able to evaluate the models more extensively.

Acknowledgements. This comparison would not have been possible without the financial support of the European program FP-7 ICE2SEA, grant no. 226375, and the financial and logistical support of the French polar institute IPEV (program CALVA-1013). Additional support by INSU through the LEFE/CLAPA project and OSUG through the CENACLAM/GLACIOCLIM observatory is also acknowledged. We would like to thank all the on-site personnel in Dumont D'Urville and Cap Prud'homme for their help. We acknowledge the Idris Computing Center for proving computer time.

References

Agosta, C., Favier, V., Genthon, C., Gallée, H., Krinner, G., Lenaerts, J. T. M., and van den Broeke, M. R.: A 40-year accumulation dataset for Adélie Land, Antarctica and its application for model validation, Clim. Dynam., 38, 75–86, doi:10.1007/s00382-011-1103-4, 2012.

Andreas, E. L.: A Physically Based Model of the Form Drag Associated with Sastrugi, CRREL Report No CR95-16, NTIS, Springfield, 1995.

Bintanja, R.: Snowdrift suspension and atmosphéric turbulence. Part 1: theoretical background and model description, Bound.-Lay. Meteorol., 95, 343–368, 2000.

Brasseur, O., Gallée, H., Boyen, H., and Tricot, C.: Reply to "Comments on Development and Application of a Physical Approach to estimating Wind Gust, Mon. Weather Rev., 130, 1936–1942, 2002.

Budd, W. F.: The drifting of nonuniform snow particles, in: Studies in Antarctic Meteorology, Vol. 9, 59–70, AGU, Washington, D. C., 1966.

Budd, W. F., Dingle, W. R. J., and Radok, U.: The Byrd snow drift project outline and basic results, in: Studies in Antarctic Meteorology, Antarctic Research Series, edited by: Rubin, M. J., American Geophysical Union, Washington, D. C., 71–134, 1966.

Cierco, F.-X., Naaim-Bouvet, F., and Bellot, H.: Acoustic sensors for snowdrift measurements: How should they be used for research purposes?, Cold Reg. Sci. Technol., 49, 74–87, doi:10.1016/j.coldregions.2007.01.002, 2007.

Déry, S. J. and Yau, M. K.: Large-scale mass balance effects of blowing snow and surface sublimation, J. Geophys. Res., 107, 1–8, doi:10.1029/2001JD001251, 2002.

Doorschot, J. J. J. and Lehning, M.: Equilibriul saltation: mass fluxes, aerodynamic entrainment, and dependence on grain properties, Bound.-Lay. Meteorol., 104, 111–130, 2002.

Favier, V., Agosta, C., Genthon, C., Arnaud, L., Trouvilliez, A., and Gallée, H.: Modeling the mass and surface heat budgets in a coastal blue ice area of Adélie Land, Antarctica, J. Geophys. Res., 116, F03017, doi:10.1029/2010JF001939, 2011.

Gallée, H. and Gorodetskaya, I. V.: Validation of a limited area model over Dome C, Antarctic Plateau, during winter, Clim. Dynam., 34, 61–72, doi:10.1007/s00382-008-0499-y, 2010.

Gallée, H. and Schayes, G.: Development of a three-dimensional meso-γ primitive equation model: katabatic winds simulation in the area of Terra Nova Bay, Antarctica, Mon. Weather Rev., 122, 671–685, 1994.

Gallée, H., Guyomarc'h, G., and Brun, É.: Impact of snow drift on the antarctic ice sheet surface mass balance: possible sensitivity to snow-surface properties, Bound.-Lay. Meteorol., 99, 1–19, 2001.
Gallée, H., Peyaud, V., and Goodwin, I.: Simulation of the net snow accumulation along the Wilkes Land transect, Antarctica, with a regional climate model, Ann. Glaciol., 41, 1–6, 2005.
Gallée, H., Trouvilliez, A., Agosta, C., Genthon, C., Favier, V., and Naaim-Bouvet, F.: Transport of snow by the wind: a comparison between observations in Adélie Land, Antarctica, and simulations made with the regional climate model MAR, Bound.-Lay. Meteorol., 146, 133–147, doi:10.1007/s10546-012-9764-z, 2013.
Garcia, R.: Mesures de transport de neige par le vent à la station Charcot, La météorologie, 57, 205–213, 1960.
Garratt, J. R.: The Atmospheric Boundary Layer, Cambridge Atmospheric and Space Science Series, Cambridge University Press, Cambridge, 1992.
Genthon, C., Lardeux, P., and Krinner, G.: The surface accumulation and ablation of a coastal blue-ice area near Cap Prudhomme, Terre Adélie, Antarctica, J. Glaciol., 53, 635–645, 2007.
Goff, J. A. and Gratch, S.: Low-pressure properties of water from −160 °F to 212 °F, Trans. Am. Soc. Heat. Vent. Eng., 52, 95–121, 1946.
Gordon, M., Biswas, S., Taylor, P. A., Hanesiak, J., Albarran-Melzer, M., and Fargey, S.: Measurements of drifting and blowing snow at Iqaluit, Nunavut, Canada during the star project, Atmos. Ocean, 48, 81–100, doi:10.3137/AO1105.2010, 2010.
Guyomarc'h, G. and Mérindol, L.: Validation of an application for forecasting blowing snow, Ann. Glaciol., 26, 138–143, 1998.
Jackson, B. S. and Carroll, J. J.: Aerodynamic roughness as a function of wind direction over asymmetric surface elements, Bound.-Lay. Meteorol., 14, 323–330, 1978.
Kotlyakov, V. M.: Results of a study of the processes of formation and structure of the upper layer of the ice sheet in Eastern Antarctica, in Symposium on Antarctic Glaciology, 88–99, IAHS Publication, Helsinki., 1961.
Lenaerts, J. T. M., van den Broeke, M. R., Déry, S. J., König-Langlo, G., Ettema, J., and Munneke, P. K.: Modelling snowdrift sublimation on an Antarctic ice shelf, The Cryosphere, 4, 179–190, doi:10.5194/tc-4-179-2010, 2010.
Lenaerts, J. T. M., Van Den Broeke, M. R., van de Berg, W. J., van Meijgaard, E., and Kuipers Munneke, P.: A new, high-resolution surface mass balance map of Antarctica (1979–

2010) based on regional atmospheric climate modeling, Geophys. Res. Lett., 39, 1–5, doi:10.1029/2011GL050713, 2012a.

Lenaerts, J. T. M., van den Broeke, M. R., Déry, S. J., van Meijgaard, E., van de Berg, W. J., Palm, S. P., and Sanz Rodrigo, J.: Modeling drifting snow in Antarctica with a regional climate model: 1. Methods and model evaluation, J. Geophys. Res., 117, D05108, doi:10.1029/2011JD016145, 2012b.

Lenaerts, J. T. M., Van Den Broeke, M. R., Scarchilli, C., and Agosta, C.: Impact of model resolution on simulated wind, drifting snow and surface mass balance in Terre Adélie, East Antarctica, J. Glaciol., 58, 821–829, doi:10.3189/2012JoG12J020, 2012c.

Leonard, K. C., Tremblay, L.-B., Thom, J. E., and MacAyeal, D. R.: Drifting snow threshold measurements near McMurdo station, Antarctica: a sensor comparison study, Cold Reg. Sci. Technol., 70, 71–80, doi:10.1016/j.coldregions.2011.08.001, 2011.

Lorius, C.: Contribution to the knowledge of the Antarctic ice sheet: a synthesis of glaciological measurements in Terre Adélie, J. Glaciol., 4, 79–92, 1962.

Madigan, C. T.: Meteorology. Tabulated and reduced records of the Cape Denison Station, Adélie Land. Australasian Antarctic Expedition 1911–1914 Scientific Reports, Serie B, Vol. 4., 1929.

Mann, G. W., Anderson, P. S., and Mobbs, S. D.: Profile measurements of blowing snow at Halley, Antarctica, J. Geophys. Res., 105, 24491–24508, doi:10.1029/2000JD900247, 2000.

Marticorena, B. and Bergametti, G.: Modeling the atmospheric dust cycle: 1. Design of a soil-derived dust emission scheme, J. Geophys. Res., 100, 16415–16430, 1995.

Naaim-Bouvet, F., Bellot, H., and Naaim, M.: Back analysis of drifting-snow measurements over an instrumented mountainous site, Ann. Glaciol., 51, 207–217, doi:10.3189/172756410791386661, 2010.

Nash, J. E. and Sutcliffe, J. V.: River flow forecansting through conceptual models Part 1 – A discussion of principles, J. Hydrol., 10, 282–290, 1970.

Owen, P. R.: Saltation of uniform grains in air, J. Fluid Mech., 20, 225–242, 1964.

Palerme, C., Kay, J. E., Genthon, C., L'Ecuyer, T., Wood, N. B., and Claud, C.: How much snow falls on the Antarctic ice sheet?, The Cryosphere, 8, 1577–1587, doi:10.5194/tc-8-1577-2014, 2014.

Palm, S. P., Yang, Y., Spinhirne, J. D., and Marshak, A.: Satellite remote sensing of blowing snow properties over Antarctica, J. Geophys. Res., 116, 1–16, doi:10.1029/2011JD015828, 2011.

TCD
8, 6007–6032, 2014

Parish, T. R. and Wendler, G.: The katabatic wind regime at Adélie Land, Antarctica, Int. J. Climatol., 11, 97–107, 1991.

Pomeroy, J. W.: A process-based model of snow drifting, J. Glaciol., 13, 237–240, 1989.

Pomeroy, J. W. and Male, D. H.: Steady-state suspension of snow, J. Hydrol., 136, 275–301, doi:10.1016/0022-1694(92)90015-N, 1992.

Prud'homme, A. and Valtat, B.: Les observations météorologiques en Terre Adélie 1950–1952 – Analyse critique, Expéditions polaires françaises, Paris, 1957.

Radok, U.: Snow Drift, J. Glaciol., 19, 123–139, 1977.

Scarchilli, C., Frezzotti, M., Grigioni, P., De Silvestri, L., Agnoletto, L., and Dolci, S.: Extraordinary blowing snow transport events in East Antarctica, Clim. Dynam., 34, 1195–1206, doi:10.1007/s00382-009-0601-0, 2010.

Sørensen, M.: An analytic model of wind-blown sand transport, in Acta Mechanica (Suppl.), Vol. 1, edited by: Barndorff-Nielsen, O. and Willetts, B., 1–19, Springer, Vienna, 1991.

Trouvilliez, A., Naaim-Bouvet, F., Genthon, C., Luc, P., Favier, V., Bellot, H., Agosta, C., Palerme, C., Amory, C., and Gallée, H.: A novel experimental study of aeolian snow transport in Adélie Land (Antarctica), Cold Reg. Sci. Technol., 108, 125–138, doi:10.1016/j.coldregions.2014.09.005, 2014.

Trouvilliez, A., Naaim-Bouvet, F., Bellot, H., Genthon, C., and Gallée, H.: Evaluation of Flowcapt acoustic sensor for snowdrift measurements, J. Atmos. Ocean. Tech., submitted, 2014.

Wamser, C. and Lykossov, V. N.: On the friction velocity during blowing snow, Contrib. to Atmos. Phys., 68, 85–94, 1995.

Wendler, G.: On the blowing snow in Adélie Land, eastern Antarctica. A contribution to I. A. G.O, in: Glacier fluctuations and climatic change, edited by: Oerlemans, J., 261–279, Kluwer Academic Publishers, Reidel, Dodrecht, 1989.

Wendler, G., Stearns, C. R., Dargaud, G., and Parish, T. R.: On the extraordinary katabatic winds of Adélie Land, J. Geophys. Res., 102, 4463–4474, 1997.

Wilkinson, R. H.: A Method for Evaluating Statistical Errors Associated with Logarithmic Velocity Profiles, Geo.-Mar. Lett., 3, 49–52, 1984.

Xiao, J., Bintanja, R., Déry, S. J., Mann, G. W., and Taylor, P. A.: An intercomparison among four models of blowing snow, Bound.-Lay. Meteorol., 97, 109–135, 2000.

Table 1. Localisation and description of the automatic weather and snow stations installed in Adélie Land.

	D3	D17	D47
Localisation	66.694 S, 139.898 E, 110 m a.s.l.	66.724 S, 139.706 E, 465 m a.s.l.	67.393 S, 138.709 E, 1565 m a.s.l.
Since	Feb 2009	Feb 2010	Jan 2010
Atmospheric measurements	Wind speed, temperature and hygrometry at 2 m	Wind speed, temperature and hygrometry at 6 levels	Wind speed, temperature and hygrometry at 2 m
Blowing snow measurements	First generation FlowCapt^{TM} from 0 to 1, 1 to 2 and 2 to 3 m	Second generation FlowCapt^{TM} from 0 to 1 m	Second generation FlowCapt^{TM} from 0 to 1 and 1 to 2 m

TCD
8, 6007–6032, 2014

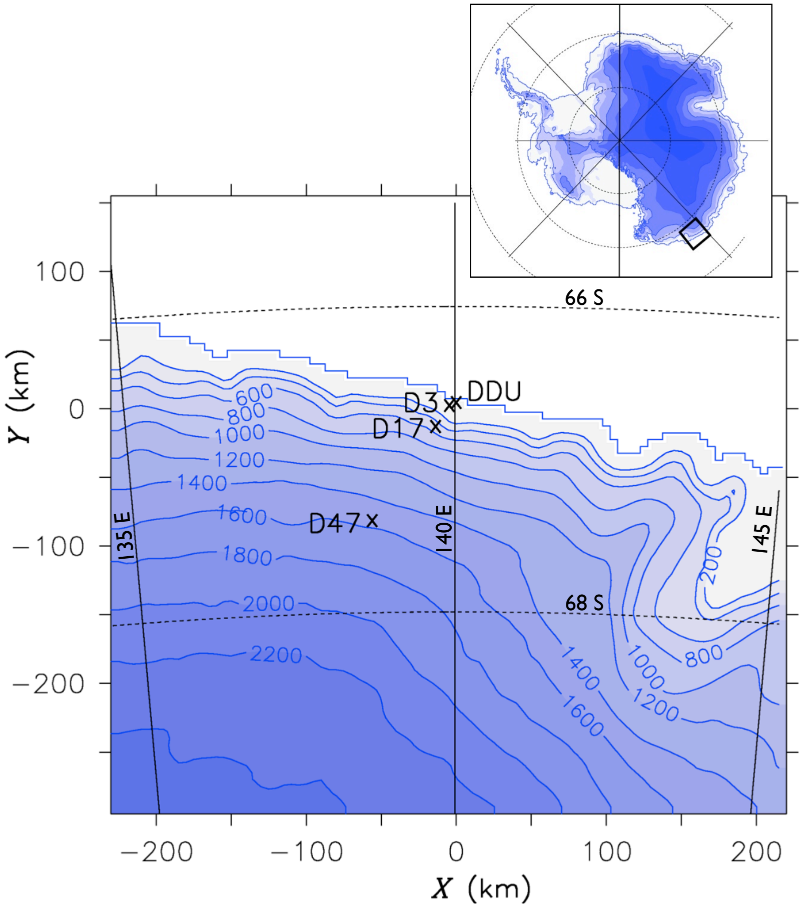

Figure 1. Integrative domain of the MAR in Adélie Land, East Antarctica. Crosses represent the Dumont D'Urville station (DDU), two automatic weather and snow stations used in this study (D17 and D47) and D3, which was the former station used in Gallée et al. (2013).

TCD
8, 6007–6032, 2014

Comparison of aeolian snow transport events and snow mass fluxes

A. Trouvilliez et al.

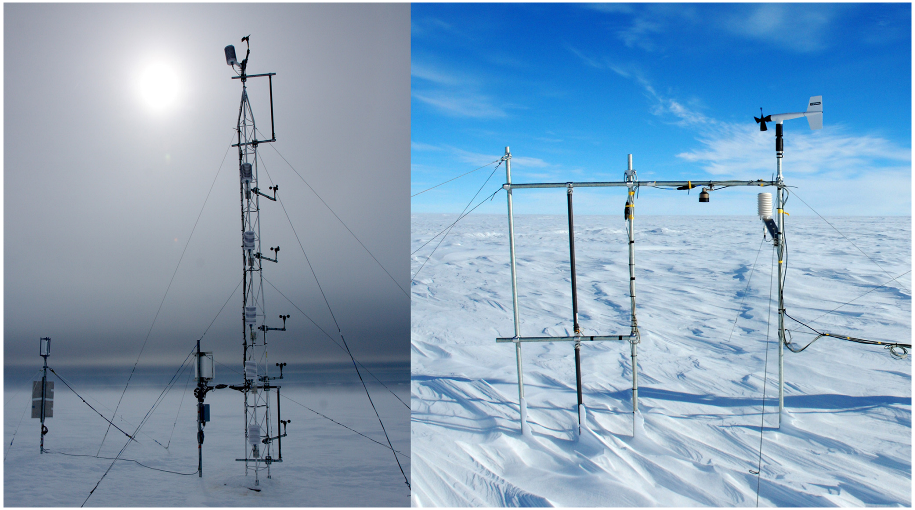

Figure 2. Left: the D17 7 m mast with one second-generation FlowCapt^{TM} and Right: the D47 automatic weather and snow station with two second-generation FlowCapt^{TM} sensors.

TCD
8, 6007–6032, 2014

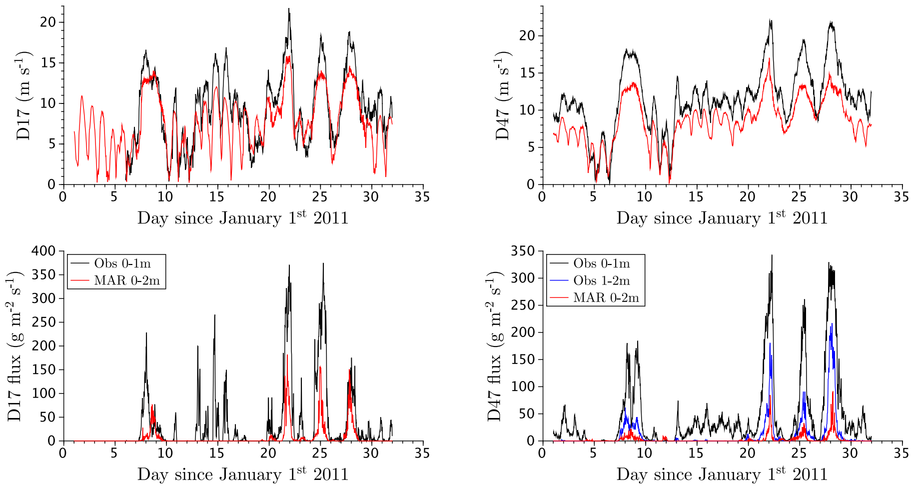

Figure 3. Top: observed (black) and simulated (red) wind speed at 2 m height. Bottom: aeolian snow transport events comparison between observed snow mass fluxes from 0 to 1 m (black) and simulated ones from 0 to 2 m (red) for the D17 site (bottom left) and the D47 site (bottom right). The observed snow mass fluxes from 1 to 2 m (blue) are also represented for the D47 site.

TCD
8, 6007–6032, 2014

Comparison of aeolian snow transport events and snow mass fluxes

A. Trouvilliez et al.

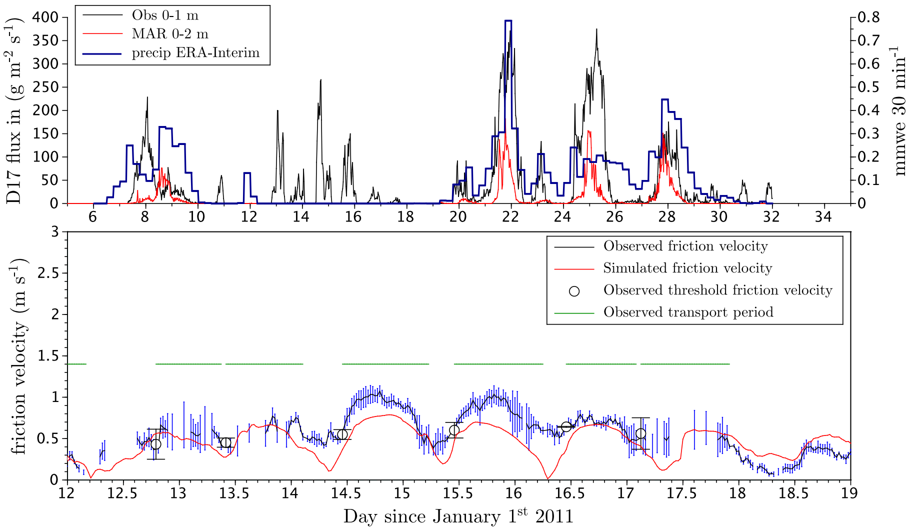

Figure 4. Top: comparison of aeolian snow transport events between observed snow mass fluxes from 0 to 1 m (black), simulated ones from 0 to 2 m (red) and precipitation from ERA-interim for the D17 site. Bottom: observed friction velocity (black line) at D17 and observed threshold friction velocity (black dot). The blue bars represent the 95 % confidence limit of the friction velocity. The horizontal green bar represents the observed aeolian snow transport periods numbered from 1 to 6.

TCD
8, 6007–6032, 2014

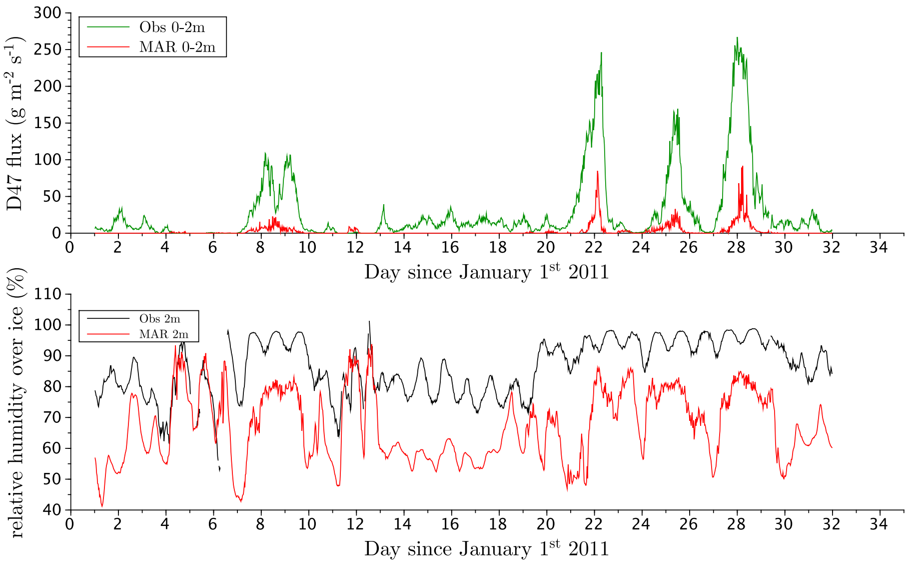

Figure 5. Top: observed (green) and simulated (red) snow mass fluxes from 0 to 2 m. Bottom: observed (black) and simulated (red) relative humidity over ice at 2 m.

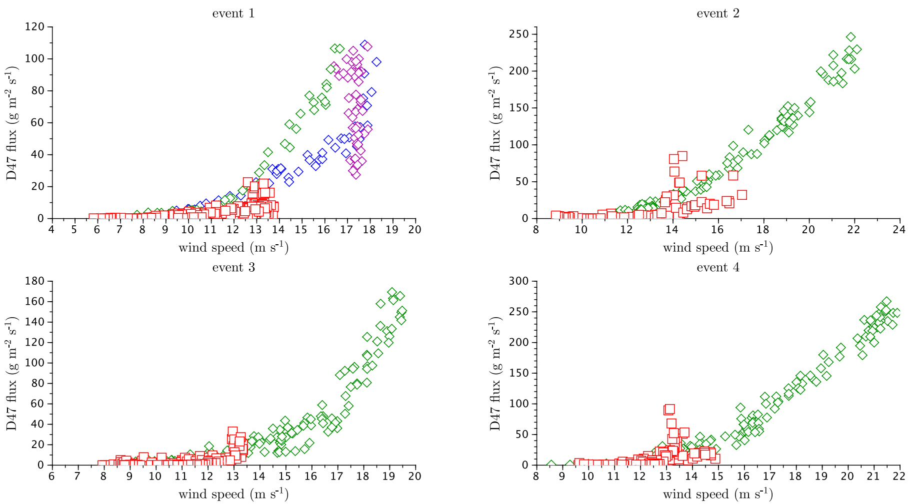

Figure 6. Observed (diamond) and simulated (red square) snow mass fluxes vs. the observed (and simulated respectively) wind speed in January 2011 from 0 to 2 m for the four strong aeolian snow transport events. Event 1 is from the 7th to the 10th, event 2 from the 21th to the 22th, event 3 from the 24th to the 26th and event 4 from the 27th to the 29th. For the first event, the observed snow mass fluxes are decomposed in time between a first (blue), an intermediate (purple) and a final relationship (green).